12-2020

System Level Characterization of the Gridded Retarding Ion Drift Sensor (GRIDS) for the PetitSat Mission

Benjamin B. Oborn
Utah State University

SYSTEM LEVEL CHARACTERIZATION OF THE GRIDDED RETARDING ION DRIFT SENSOR (GRIDS) FOR THE PETITSAT MISSION

by

Benjamin B. Oborn

A thesis submitted in partial fulfillment
of the requirements for the degree

of

MASTER OF SCIENCE

in

Electrical Engineering

Approved:

Ryan L. Davidson, Ph.D. Major Professor	Charles M. Swenson, Ph.D. Committee Member
Todd K. Moon, Ph.D. Committee Member	D. Richard Cutler, Ph.D. Interim Vice Provost for Graduate Studies

UTAH STATE UNIVERSITY
Logan, Utah

2020

ABSTRACT

System Level Characterization of the Gridded Retarding Ion Drift Sensor (GRIDS) for the PetitSat Mission

by

Benjamin B. Oborn, Master of Science

Utah State University, 2020

Major Professor: Ryan L. Davidson, Ph.D.
Department: Electrical and Computer Engineering

PetitSat is a cube satellite (CubeSat) mission engineered to collect in situ measurements of plasma and neutral particles in Earth's ionosphere. The measurements taken by PetitSat will propel the scientific community closer to prediction of ionospheric weather. The ability to predict when and where weather phenomenon will occur will assist in avoiding negative consequences that can result from the phenomenon. Once such negative consequence is satellite and over-the-horizon communications disruptions. To collect these measurements, one of the instruments on PetitSat is a unique combination of two legacy instruments. They are a retarding potential analyzer (RPA) and an ion drift meter (IDM). Together they are dubbed the Gridded Retarding Ion Drift Sensor (GRIDS). The purpose of this thesis is a system level characterization of the GRIDS firmware and hardware. Characterizing the instrument is essential to show its suitability for use on PetitSat and to enable correct interpretation of the data it generates.

(57 pages)

PUBLIC ABSTRACT

System Level Characterization of the Gridded Retarding Ion Drift Sensor (GRIDS) for the PetitSat Mission

Benjamin B. Oborn

Weather prediction, wherever people live, serves as a beneficial part of everyday life. Weather in the upper portions of Earth's atmosphere also impacts life on Earth but it is not able to be predicted as well as its terrestrial counterpart. PetitSat is a cube satellite (CubeSat) mission proposed to help remedy this issue. It will collect measurements of charged particles in the upper atmosphere called a plasma. The measurements taken by PetitSat will facilitate better prediction of upper-atmospheric weather. Prediction of when and where weather phenomenon will occur will allow avoidance of negative consequences that can result. Once such negative consequence is satellite and over-the-horizon communications interference.

In order to collect these measurements, one of the instruments on PetitSat is a unique combination of two time-tested instruments. The instruments are a retarding potential analyzer (RPA) and an ion drift meter (IDM). Together, they are called the Gridded Retarding Ion Drift Sensor (GRIDS). Work has been done previously in developing firmware and hardware for GRIDS. This thesis' purpose is to document the system level characterization of GRIDS. This will allow the data eventually gathered by GRIDS to be correctly interpreted and show its suitability for the PetitSat mission.

To my family.

ACKNOWLEDGMENTS

Many thanks go to Dr. Davidson for his patience and mentoring. He has facilitated my being able to provide for my family for the rest of my life through the skills and lessons learned. While I owe thanks to many, I'm particularly grateful for his help.

Benjamin B. Oborn

CONTENTS

LIST OF TABLES

LIST OF FIGURES

ACRONYMS

ADC	Analog-to-Digital Converter
BRAM	Block Random Access Memory
CRC	Cyclic Redundancy Check
CubeSat	Cube Satellite
DAC	Digital-to-Analog Converter
EMI	ElectroMagnetic Interference
ETU	Engineering Test Unit
FPGA	Field Programmable Gate Array
GRIDS	Gridded Retarding Ion Distribution Sensor
IDM	Ion Drift Meter
IRI	International Reference Ionosphere
ISS	International Space Station
MSTID	Medium-Scale Traveling Ionosphere Disturbance
NASA	National Aeronautics and Space Administration
NMS	Neutral Mass Spectrometer
PetitSat	Plasma Enhancements in The Ionosphere-Thermosphere Satellite
PVVISS	Plasma Velocity Vector Instrument for Small Satellites
RPA	Retarding Potential Analyzer
SWaP	Size, Weight, and Power
TRL	Technology Readiness Level
USU	Utah State University
VHDL	VHSIC Hardware Description Language
VHSIC	Very High-Speed Integrated Circuit
VT	Virginia polyTechnic Institute and State University

CHAPTER 1

INTRODUCTION

Predicting terrestrial weather in the lower atmosphere can inform humankind of an incoming hurricane, a dangerous tornado, torrential rain or driving snow. Collecting data for terrestrial weather happens regularly and in high quantities. More data lends itself to improved understanding of the physics driving weather patterns and, consequently, better predictive models with higher levels of predictive accuracy. Weather in the upper atmosphere is not presently as well understood as its terrestrial counterpart nor are the links between the two fully known. This is due in part to lower data collection and different physical phenomenon stimulating behavior.

The ionosphere plays an important role in the conditions in the upper atmosphere and presents its own class of potentially adverse consequences [1]. One such consequence is the blocking or degradation of satellite and over-the-horizon communication. When this occurs, it hinders the flow of navigation, intelligence, and communication information for commercial and military endeavors [2]. Plasma density irregularities – specifically increases in density - are one cause of these disruptions. Increased density in the charged particles comprising the plasma in the ionosphere are called enhancements or plasma blobs, while areas of decreased plasma density are called depletions or bubbles. Both phenomena can distort radio waves, corrupting or impeding the transmission of information.

Many studies dealing with plasma density irregularities focus on characterizing the irregularities without quantifying the relative contribution of their drivers. For example, blobs are thought to have two main drivers, bubbles and Medium-Scale Traveling Ionosphere Disturbances (MSTIDs) [3]. It is not definitively known, however, which contributes more and when. The question arises, "What is needed to better understand the contributing factors producing plasma density enhancements and, like terrestrial weather, move toward accurate prediction of when they will occur?" The path from observation to prediction lies in

the collection and analysis of data about the creation of blobs. Much of this data collection must occur where the irregularities occur – the ionosphere.

1.1 PetitSat

The Plasma Enhancements in the Ionosphere-Thermosphere Satellite (PetitSat) [4] is a 6U cube satellite (CubeSat) mission engineered to collect in-situ measurements of plasma density enhancements. It was selected by NASA in Spring of 2017 and is preparing to launch in the Fall of 2021. It will launch to the International Space Station (ISS) where it will then be deployed and begin its six-month mission. The ISS orbit conveniently provides a suitable orbit for PetitSat. With an altitude of approximately 400 km and inclination of 51°, PetitSat will pass through the F-peak, a section of the ionosphere that has the highest ion density, and will span low- to mid-latitudes of the Earth. These orbit attributes allow PetitSat to sample a portion of the ionosphere where many plasma density irregularities occur and in latitudes not covered by previous satellites like C/NOFS.

The overarching questions to be answered by PetitSat's mission are:

1. What is the observed drift, density, and O^+, He^+, and H^+ signatures of plasma enhancements as a function of magnetic latitude?

2. What is the relative contribution of MSTIDs to the generation of plasma enhancements in the ionosphere?

Answering these questions will help forecast plasma irregularities and connect MSTIDs and enhancements together. Enabling these questions to be answered is the job of the two instruments on-board PetitSat. The first is called the Neutral Mass Spectrometer (NMS) and the second is called the Gridded Retarding Ion Drift Sensor (GRIDS) [5].

The NMS is used for gathering information about the neutral particles in the thermosphere; in particular, their masses and densities. With one exception, the NMS is a copy of an instrument that flew on experiments called ExoCube [6] and Dellingr [7]. It was developed jointly by NASA and California Polytechnic State University. The original instrument

had an additional capability to measure ion densities. This capability will be removed on PetitSat as GRIDS will perform this function.

GRIDS is a unique amalgamation of two historically successful instruments. They are the Retarding Potential Analyzer (RPA) [8] and the Ion Drift Meter (IDM) [9].

An RPA can measure several ionospheric parameters simultaneously including ion concentration, ion temperature, ion mass ratios, and ion drift velocity in the ram direction. Few instruments can measure such a wide variety of phenomenon in one package.

Unlike the RPA, an IDM cannot measure the velocity of incoming ions in the ram direction. An IDM is made specifically to measure the transverse velocities of ions. This allows the combination of an RPA and IDM to characterize the three-dimensional movement of the ions they are immersed in. For GRIDS, the combination of these instruments creates a simple but versatile instrument that will help PetitSat characterize the ionosphere and potentially link MSTIDs and plasma enhancements.

Two parties are primarily responsible for the GRIDS instrument. Utah State University (USU) has designed, developed, and tested the hardware and firmware for GRIDS. Virginia Polytechnic and State University (VT) will lead the calibration and vacuum chamber testing campaign. The purpose of this thesis is to detail what was undertaken by USU to characterize GRIDS on a system level and take the GRIDS Engineering Test Unit (ETU) from test configuration to flight-ready status. The ETU is the functional prototype and precursor of the final flight unit. The ETU provides a way to identify and correct mistakes in the GRIDS design as well as perform much of the testing that will demonstrate the functionality of instrument prior to launch. The ETU is currently rated as being at a technology readiness level (TRL) of 5. A TRL of 5 means GRIDS is a working prototype that requires further testing in an environment similar to the environment it will be in when GRIDS orbits the Earth. The vacuum chamber at VT will provide such an environment. Therefore, upon successful completion of vacuum chamber testing, GRIDS will move to TRL 6.

Fig. 1.1 shows the checkpoints necessary to take the ETU from test to flight status. Before being considered flight worthy, GRIDS must pass through all the checkpoints shown.

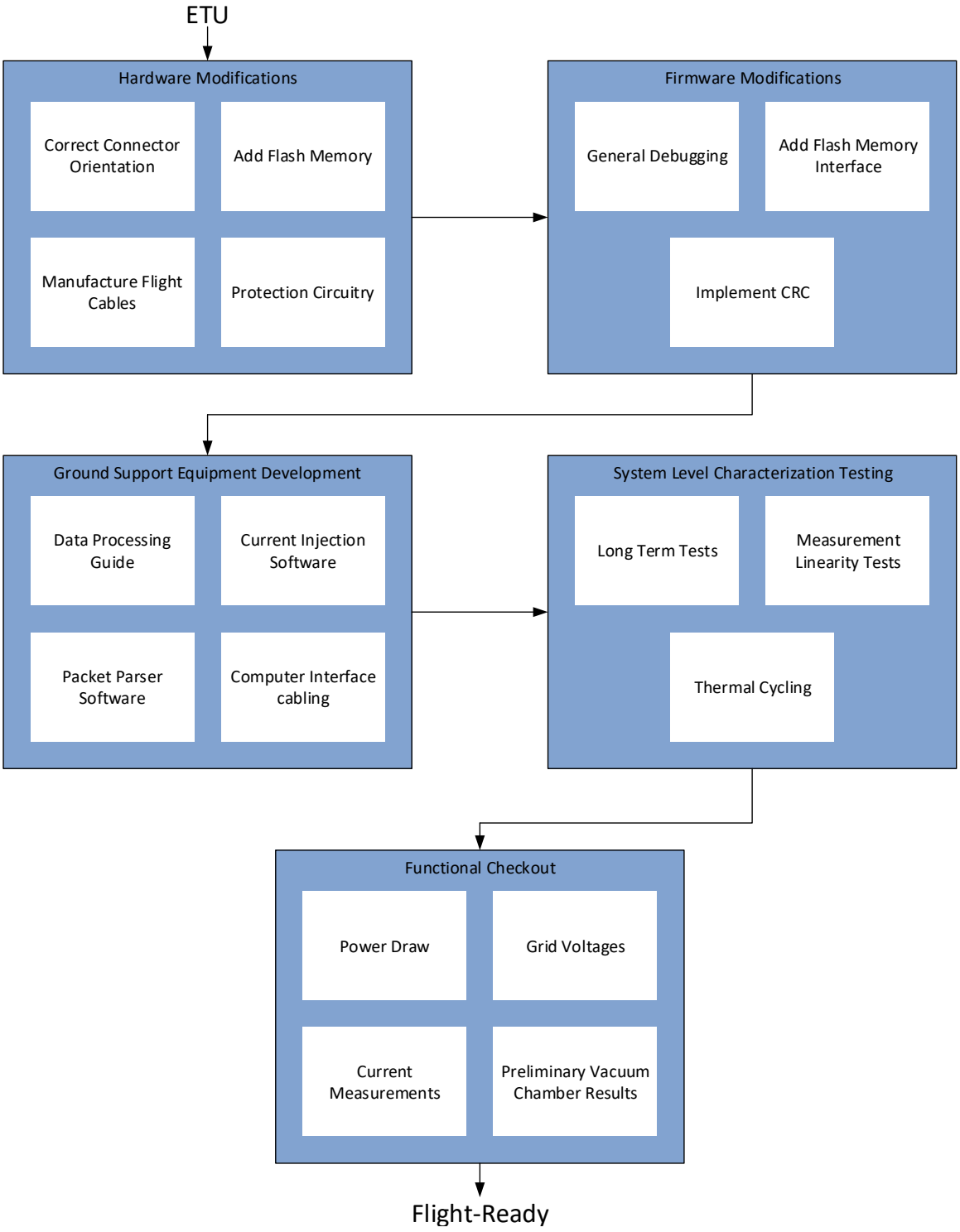

Fig. 1.1: ETU-to-Flight Checkpoints

CHAPTER 2

Background

The ionosphere contains several ion species. What species are present depends on several factors including altitude, latitude, and day- or night-side of the Earth. At the altitude of 400 km (PetitSat's orbit altitude) the dominant species are atomic oxygen (O^+), atomic nitrogen (N^+), and atomic Hydrogen (H^+) and atomic helium (He^+). Each of these elements have unique masses which gives them a distinct amount of energy. This unique energy is one way spacecraft instrumentation can distinguish between the different ion species. For example, the kinetic energy of an ion can be calculated as:

$$KE = \frac{1}{2}mv^2 \tag{2.1}$$

where KE is the kinetic energy of the ion in Joules (J), m is the mass in kilograms (kg), and v is the velocity in meters per second (m/s). Satellites in circular orbits have speeds near 7.6 km/s in the Earth-fixed frame. At 400 km altitude, the speeds of ions are only a few hundred kilometers per second. Because the speed of the satellite is much greater than the speed of the ions, a simplifying approximation can be used where the ions are considered stationary and the satellite collides with them. If this scenario is looked at from the satellite's frame of reference, it appears as though the ions are colliding with it at 7.6 km/s. This is the velocity used in calculating the energy of the particles. For example, the kinetic energy of an oxygen ion (the mass of which is near 2.656×10^{-26} kg) is approximated as:

$$\begin{aligned} KE &= \frac{1}{2}mv^2, \\ KE &= \frac{1}{2}(2.656 \times 10^{-26})(7600)^2, \\ KE &= 7.67 \times 10^{-19}\ J \end{aligned} \tag{2.2}$$

Because ions are charged, electric fields can impose a force upon them. If a far-away ion were traveling toward an infinite plate with a positive voltage on it, the force acting on the ion as it approaches the plate would slow it down or, if the voltage were high enough, repel it. The level of voltage required to do this depends on the energy of the incoming ion. If the oxygen ion discussed previously was coming toward such a fictitious plate, the ion would stop exactly at the plate's surface if the voltage was appropriate. For this to occur, the plate would need to have potential such that the potential energy of the ion at the surface of the plate equaled the kinetic energy of the ion when it was far away from the plate. Using equation 2.2, the kinetic energy of the example oxygen ion traveling at 7.6 km/s was calculated to be 7.67×10^{-19} J. Because all of the particle's energy will be converted to potential energy by the time it reaches the surface of the plate, it will have 7.67×10^{-19} J of potential energy. The potential energy of a charge is:

$$PE = qV \tag{2.3}$$

where q is the charge of the ion in Coulombs (C) and V is the voltage in volts (V). Because the charge of the ion is known and its potential energy at the surface of the plate has been calculated, the appropriate voltage to cause the particle to stop at the surface of the plate can be estimated as:

$$\begin{aligned} PE &= qV, \\ 7.67 \times 10^{-19} &= (1.602 \times 10^{-19}) \cdot V, \\ V &= \frac{7.67 \times 10^{-19}}{1.602 \times 10^{-19}}, \\ V &= 4.79\, Volts. \end{aligned} \tag{2.4}$$

Thus, the voltage necessary to repel the ion must be greater 4.79 V. Notice that the magnitude of the voltage is equal to the magnitude of the particle's potential energy in electron-volts (eV).

As noted earlier, because the ions have different masses, they will have different energies. These different energies result in the ions being repelled by different voltages. Lighter ions will be repelled with lower voltages and heavier ions will be repelled at higher voltages. These principles can be applied to build instruments that vary the voltages on, for instance, a metal-mesh grid. At lower voltages, heavier ions will continue forward and penetrate the mesh while lighter ions will be repelled. As the more massive ions pass through the mesh grid, they can be collected and measured as current. This is the basic operating principle of two legacy spacecraft instruments called the Retarding Potential Analyzer (RPA) and the Ion Drift Meter (IDM).

2.1 The RPA and IDM

Of the vast multitudes of instruments that have flown in space, the RPA and IDM have comparatively lengthy and successful histories due to their simplicity and versatility. A discussion of their similarities and differences follows as well as description of related research and fundamental studies.

2.1.1 Retarding Potential Analyzer (RPA)

An RPA can measure a variety of parameters. They include overall plasma density, ion temperature, the relative composition of ions in the plasma, and the velocity of the ions in the ram direction of the instrument [10]. The earliest predecessor to the RPA was conceived in 1959, was called an ion trap, and flew on Sputnik III [8]. It consisted of two concentric spheres, the inner sphere being much smaller than the outer. The outer sphere was a metal mesh that allowed ions to flow through it and be collected on the solid inner sphere. By sweeping the voltage on the outer sphere, the number of ions flowing through the mesh could be changed. This change was measured as a change in current.

GRIDS works in a similar manner. Rather than concentric spheres, however, it is a box with an aperture on one end and a collection plate on the opposing side. This geometry of RPA is called a planar RPA [11] and is depicted in Fig. 2.1.

As ions enter the aperture, they encounter several metal-mesh grids. The grids are

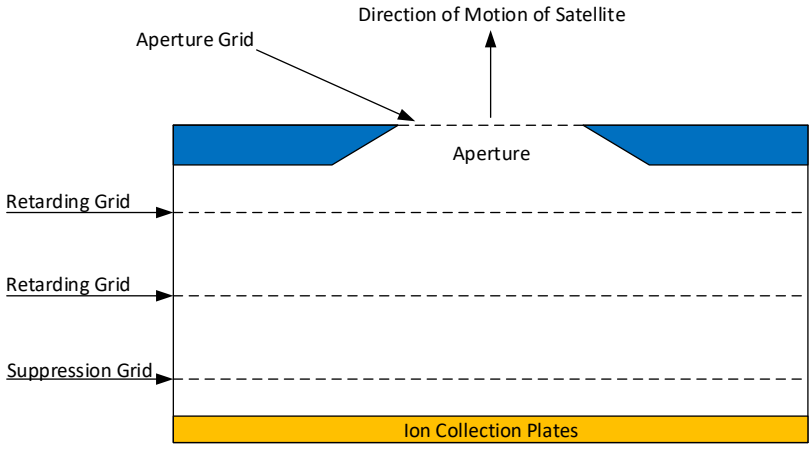

Fig. 2.1: Cross-section of a Planar RPA Instrument.

driven at differing voltages and serve different purposes. Typically, three to seven grids are used [12]. There are various names given to these grids to describe the operation they perform or their location in the grid stack. The aperture grid is the outer most grid and is typically held at the same potential as spacecraft ground and may occasionally have a small voltage applied to block lighter ions. One or more retarding grids can be found in the middle of the grid stack. The voltage on these grids is swept across a specified range of positive voltages. Just as with the ion trap, this sweep in voltage changes how much energy ions must possess in order to make it past the grid and on to the collection plate. The suppression grid is the inner most grid closest to the collector plate. It is held at a constant negative voltage. This grid is used to repel electrons. This allows only ions to hit the collector plate.

An equation used to generate a plot of current versus voltage (an I-V curve) for an ideal RPA was given by Knudsen [13] and is given in (2.5).

$$
\begin{aligned}
I &= \frac{1}{2}\chi A e v \cos\theta \sum_{i=1}^{j} n_i \left[1 + erf(k_i) + \frac{\exp(-k_i^2)}{a_i\sqrt{\pi}}\right], \\
k_i &= a_i - b, \\
a_i &= \frac{v\cos\theta}{\alpha_i}, \\
\alpha_i &= \sqrt{\frac{2k_bT}{m_i}}, \\
b &= \sqrt{\frac{e(V+\phi)}{k_bT}}.
\end{aligned}
\tag{2.5}
$$

In these equations, χ is the fractional transparency of the grid stack, A is the area of the aperture, e is the charge of an electron, v is the magnitude of the relative velocity between the satellite and the mean ion velocity, θ is the angle between the normal to the RPA aperture vector and the ion velocity vector, n_i and m_i are the number density and mass of the i^{th} ionic constituent, respectively, T is the ion temperature, V is the potential of the retarding grid relative to the spacecraft, ϕ is the potential of the spacecraft relative to the plasma, and k_b is Boltzmann's constant.

Figure 2.2 illustrates the use of Knudsen's equation to plot the current collected by an RPA. In this example, atomic oxygen, nitrogen, hydrogen and helium can be seen. Each have their own plot showing their individual contribution to the total current collected by the RPA. The plot is representative of what quantity and species of ions are present at 400 km altitude. Atomic oxygen is the most abundant at this altitude, comprising over 97% of the total ion count. nitrogen represents approximately 2%, while hydrogen and helium account for about 1% and 0.3% respectively. The lower quantity of these ions is the reason why their contribution to the total current is small. Their affects can still be seen, however, at the beginning of the plot until the voltage reaches four volts. This is where the blue "Total" plot lies on top of the plot of oxygen.

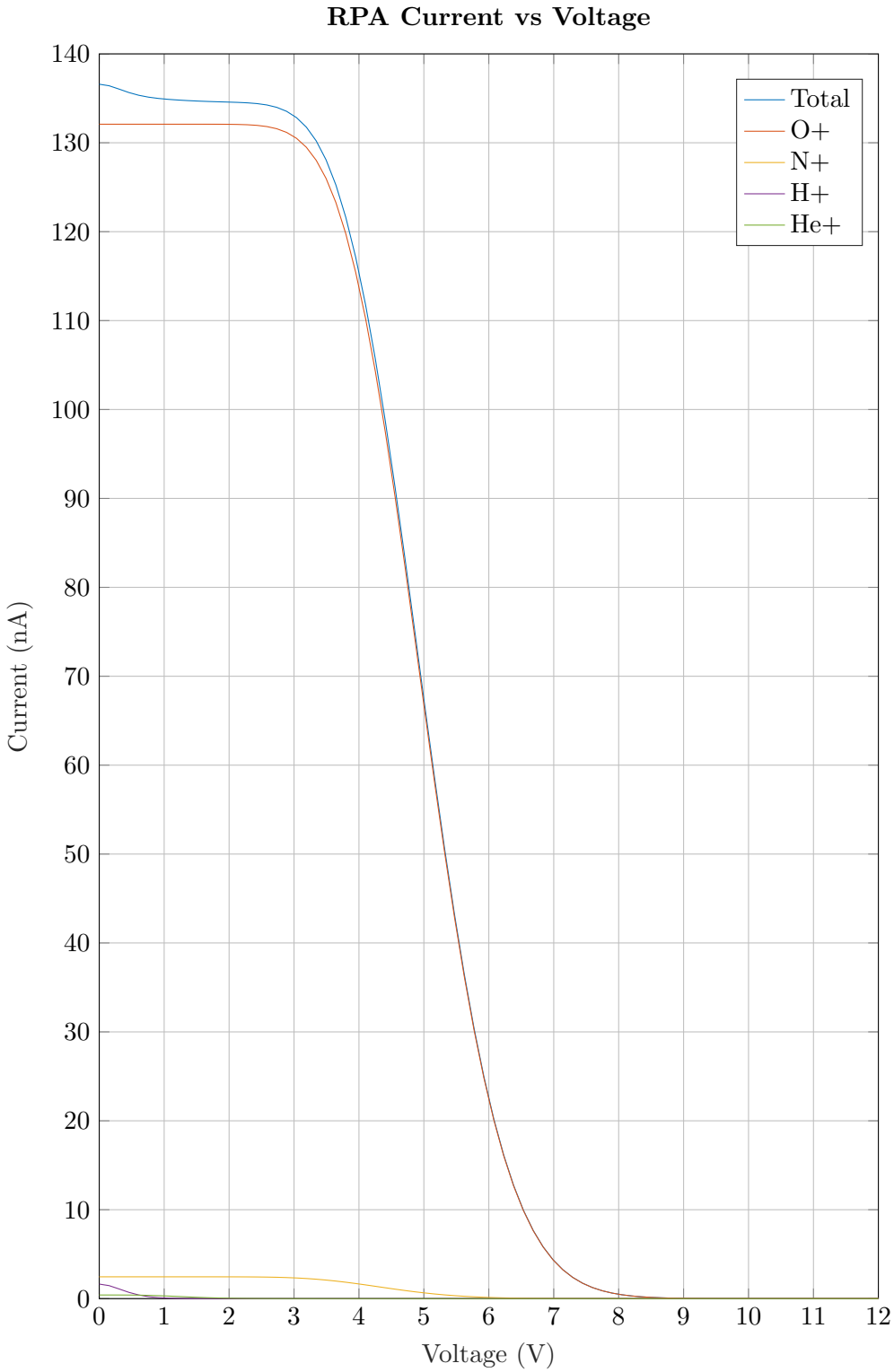

Fig. 2.2: I-V Curve at 400km Orbit

Figure 2.3 zooms in on the lower values of the plot showing the effects of increasing voltage filtering out ions from lightest to heaviest.

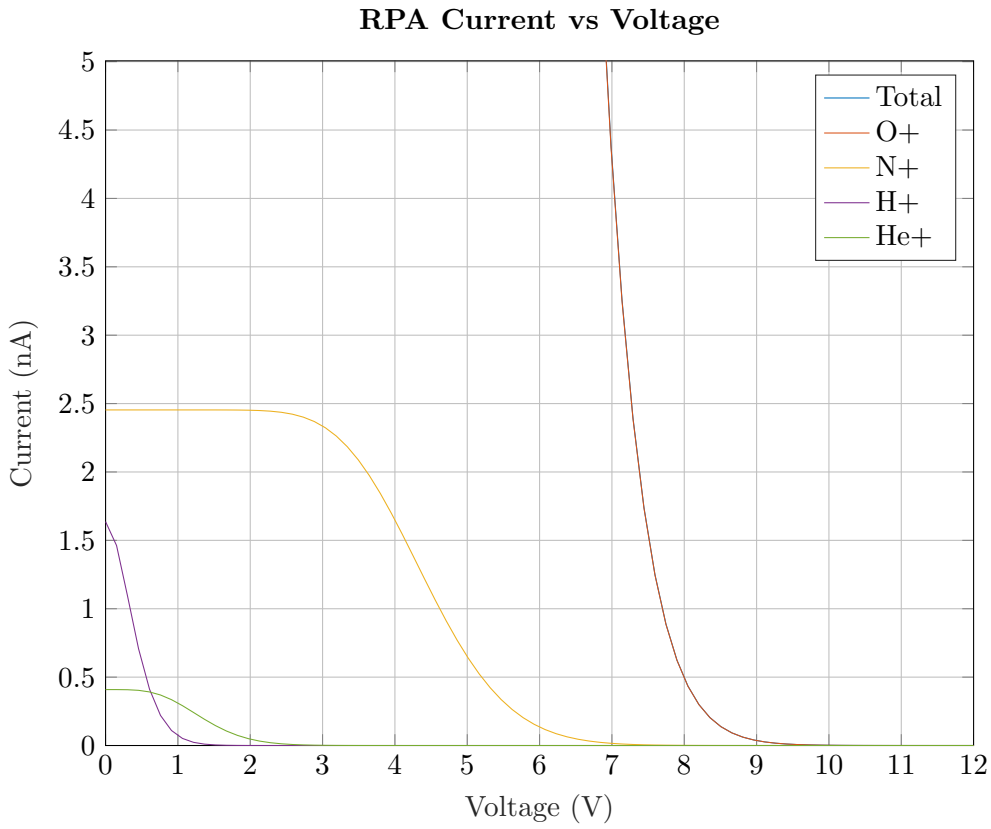

Fig. 2.3: I-V Curve at 400km Orbit Magnified

2.1.2 IDM

The function and geometry of the planar Ion Drift Meter (IDM) is similar to the RPA just described. A planar IDM geometry was first used by Hanson in the early 1970's [9]. Ions flow through an aperture, pass through grids with constant voltages on them (unlike the varying voltages of the RPA), and are collected on a collector plate opposing the aperture. On an IDM, the collector plate is divided into quadrants whereas on an RPA the collector plate is whole. The total current collected by a quadrant of the plate is described by

equation (2.6) [14].

$$I = qNA\chi V_{\perp} \tag{2.6}$$

Here, q is the charge of the incoming ions, N is the ion density, A is the illuminated area of the collector quadrant, χ is the fractional transparency of the grid stack, and $V_{\perp}$ is the velocity of the ions perpendicular to the collector plate.

Unlike an RPA, an IDM is specifically designed for gathering information about ion drift velocities perpendicular or transverse to the ram direction of the instrument. In order to determine the transverse components of the ion velocities, the collector plate of the IDM is divided into quadrants as shown in Fig. 2.4

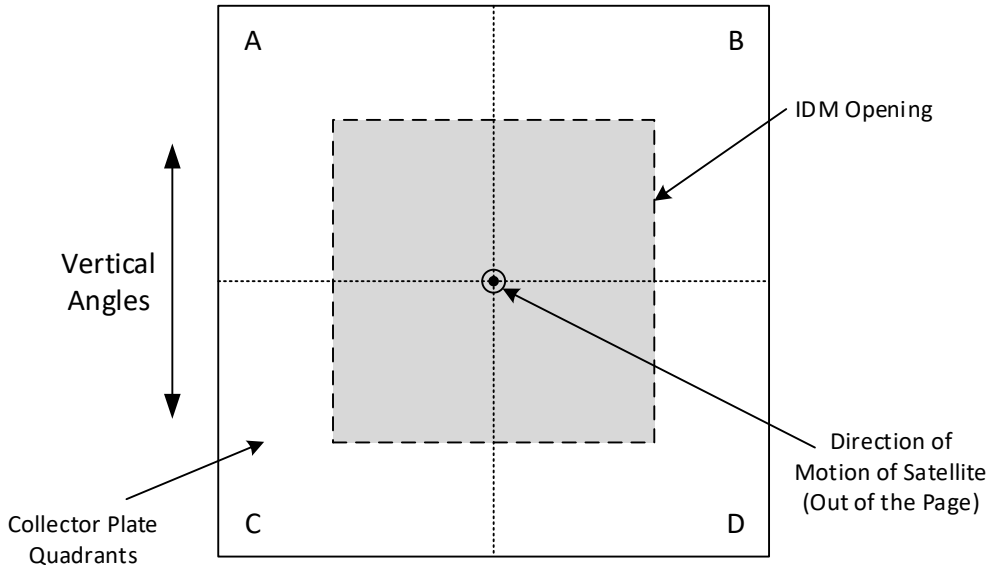

Fig. 2.4: Front View of an IDM.

As ions enter the aperture of the IDM, the transverse components of their velocities cause the ions to enter the aperture at an angle measured from a ram-pointing reference line. Fig. 2.5 illustrates this.

Depending on the angle of entry, certain quadrants of the IDM will be illuminated by the incoming ions more than others. For vertical angles, the ratio of the current collected by quadrants A and B shown in Fig. 2.4 is taken with respect to the current collected by

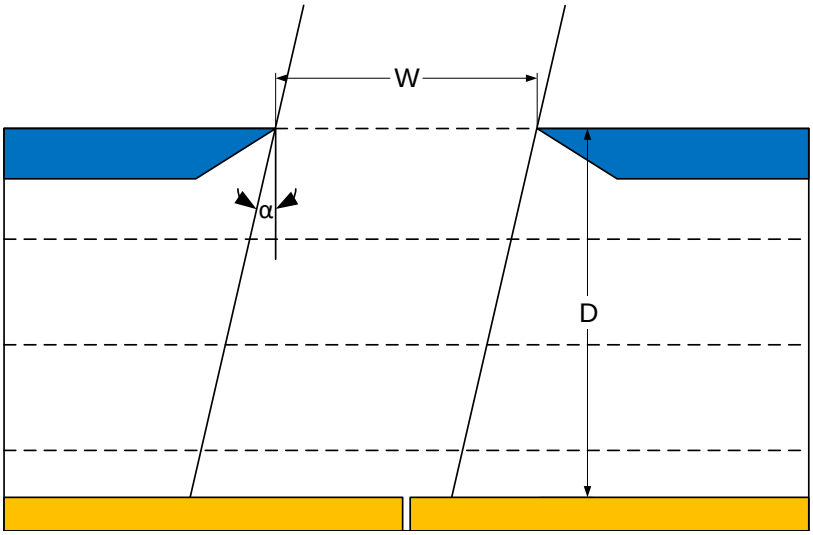

Fig. 2.5: Cross-section of an IDM.

quadrants C and D. The calculation is repeated for horizontal angles by taking the ratio of the current on the quadrants A and C with respect to the current collected by quadrants B and D. The ratio of current on the quadrants coupled with the dimensions of the IDM give sufficient information to deduce the transverse components of ion velocity. More explicitly, the equations used to calculate the entry angle are [15]:

$$\frac{I_1}{I_2} = \frac{\frac{W}{2} + D\tan\alpha}{\frac{W}{2} - D\tan\alpha} \tag{2.7}$$

Where I_1 is the current collected by one half of the detector and I_2 is the current collected by the other half, W is the width of the IDM aperture, D is the distance between the collector plate and the aperture, and α is the entry angle of the incoming ion stream. This equation can be solved for α. Thus, the measured current ratio can give the angle of entry. Solving 2.7 for α gives:

$$\alpha = \tan^{-1}\left(\frac{W\left(1 - \frac{I_1}{I_2}\right)}{2D\left(1 + \frac{I_1}{I_2}\right)}\right) \tag{2.8}$$

As mentioned previously, the voltages on the grids of an IDM are held constant. The aperture grid is held at a low, positive voltage. This repels lighter ions such as hydrogen

and helium in an attempt to isolate a single, heavier specie. The heavier ions continue through the grid stack and are collected as current. The suppression grid is held at -12 V to repel stray electrons and suppress electron emission from the collector plate.

2.1.3 RPA and IDM Combined Functionality

As demonstrated, an RPA and IDM are similar and many ways. They both consist of an aperture, stacked grids, and a collector plate. Their differences lie only in the voltages on the grids and the division of the collector plate. The sum of the collected current on the divided plates easily replicates the whole collector plate of an RPA. The voltages on the grids can be controlled through the design of the electrical hardware of the instrument. The electronics must be capable of switching between RPA mode and IDM mode. Switching between the two allows for a portion of a measurement cycle to be in RPA mode and the rest to be in IDM mode. Often, a combined RPA/IDM is sufficiently large that they are only used on bigger satellites. The size, weight, and power (SWaP) of GRIDS has specifically been designed to be compatible with a CubeSat architecture. GRIDS fits within 1U (10 cm $\times$ 10 cm $\times$ 10 cm), weighs less than a kilogram, and has power consumption of less than 1 W.

2.2 Previous Work

GRIDS has been developed with the help of several individuals. William Hatch began work on the electrical hardware of the predecessor to GRIDS, the Plasma Velocity Vector Instrument for Small Satellites (PVVISS) [10]. Many of the electronics used for PVVISS were re-used by GRIDS or provided a starting point for the GRIDS hardware. GRIDS also inherited a two-PCB design from PVVISS. The two PCBs are called the main board and the daughter board. The main board is where the majority of GRIDS electronics are found. The FPGA, voltage regulators, housekeeping electronics and communication interface electronics are all housed on the main board. The daughter board connects to the main board via a nano-d connector and is home to a four-channel, analog-to-digital converter (ADC). This ADC is responsible for measuring the current collected on each of

the four collector plates (similar to those labeled as A, B, C, and D in Fig. 2.4) used in GRIDS.

Images of the GRIDS main board and daughter board are presented in Figs. 2.6 and 2.7.

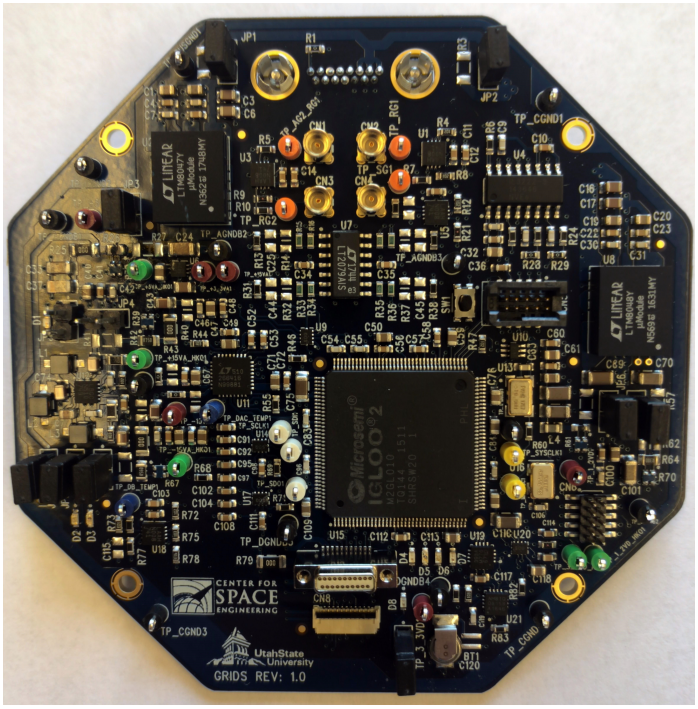

Fig. 2.6: The Completed GRIDS Main Board

The mechanical design of GRIDS was performed by Bron McCall. An image of the mechanical structure of GRIDS is shown in Figs. 2.8 and 2.9. Fig. 2.8 shows the internal grid stack as well as the mounting of the daughter board to the main board. Fig. 2.9 shows the assembled instrument. The red "Remove Before Flight" cover has been removed revealing the aperture grid used to suppress light ions in IDM mode.

The majority of FPGA firmware development was completed by Anthony Swenson [14]. He implemented VHDL to dictate when GRIDS enters RPA mode or IDM mode. He also created an algorithm that causes GRIDS to adjust its current measurement sensitivity depending on the measured current generated by incoming ions. Additionally, he imple-

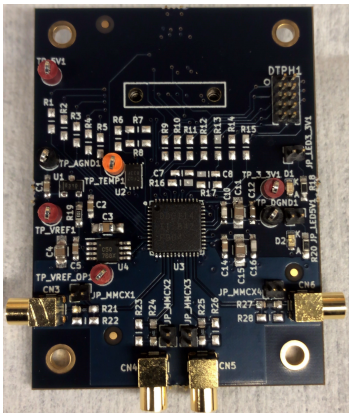

Fig. 2.7: GRIDS Daughter Board

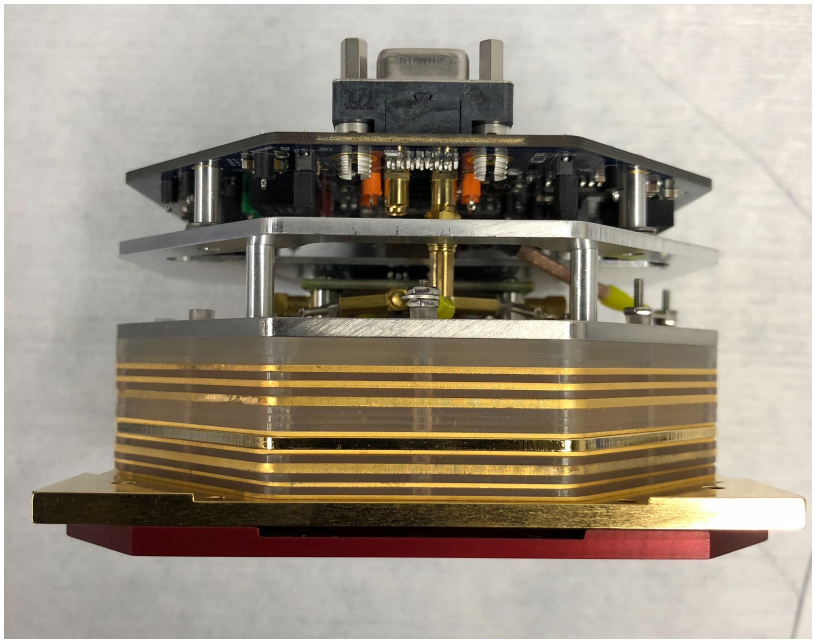

Fig. 2.8: GRIDS Internal Grid Stack-up

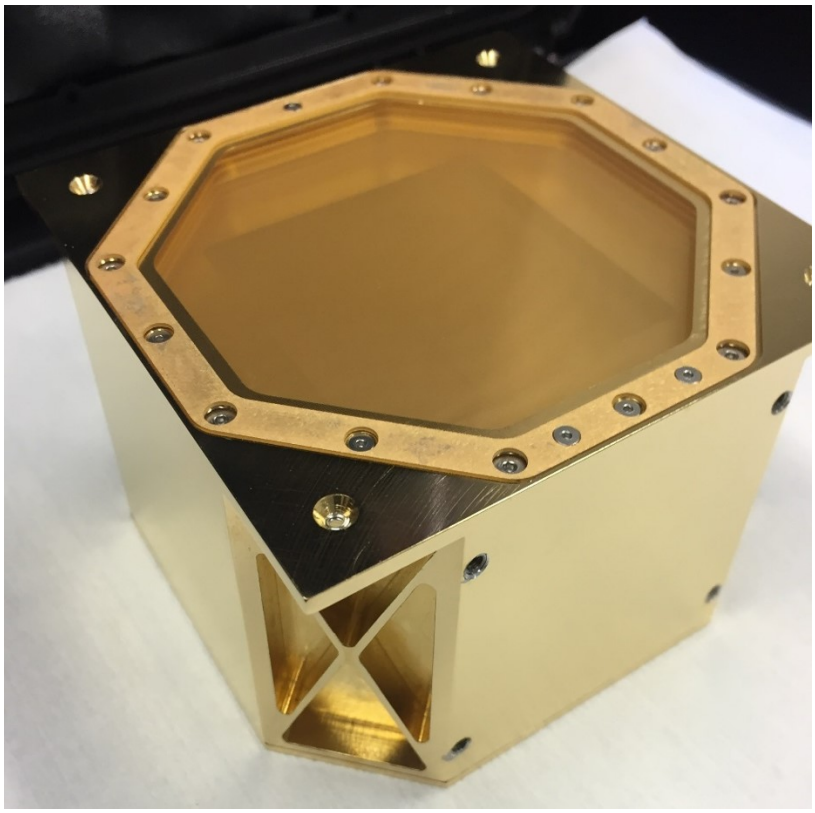

Fig. 2.9: Fully Assembled GRIDS Instrument

mented a packetizing VHDL module that puts data into a consistent packet structure used for transmitting data, a serial peripheral interface (SPI) bus, and an interface with the daughter board ADC. Some FPGA firmware design was also done by Blaine Cook. He generated VHDL to interface with a real-time clock (RTC) and made a UART module that enable communication between the FPGA and the RS422 integrated circuit (IC).

Prior to this thesis, the first generation of the GRIDS main board and daughter board had been fabricated. They became the starting point of this work and are referred to collectively as the ETU.

CHAPTER 3

System-Level Modifications and Characterization

PetitSat's mission to more fully understand the relationship between MSTIDs and plasma enhancements will only be successful if GRIDS can fulfill its role. GRIDS will be responsible for plasma velocity, temperature, density, and specie composition measurements. As such, it is critical that GRIDS fulfill its purpose and provide pertinent data. In order to assure this, characterization of the instrument must take place. Characterizing an instrument is the process of putting the instrument through many tests to understand how it performs in different circumstances and to different stimuli. The road to complete characterization passes through several checkpoints. For GRIDS, these checkpoints include modifications to hardware and firmware as well as tests of the final sensor in various circumstances. This provides assurance of proper operation and, consequently, mission success.

3.1 System-Level Modifications

Prior to initiating system level characterization of GRIDS, several modifications needed to be made to take the ETU to flight-ready status. These modifications are discussed below.

3.1.1 GRIDS Main Board

The GRIDS main board contains the majority of the electronics necessary to operate GRIDS. An image of the main board is shown in Fig. 3.1.

The main board required several hardware and firmware modifications to correct errors and make it flight-ready. An overview of the changes is enumerated and then discussed in further detail. The modifications included:

1. Correction of misplaced pin signal assignments on the Real-Time Clock (RTC) integrated circuit (IC) and a reset switch.

2. Addition of a FLASH memory IC and FPGA firmware to interface with it

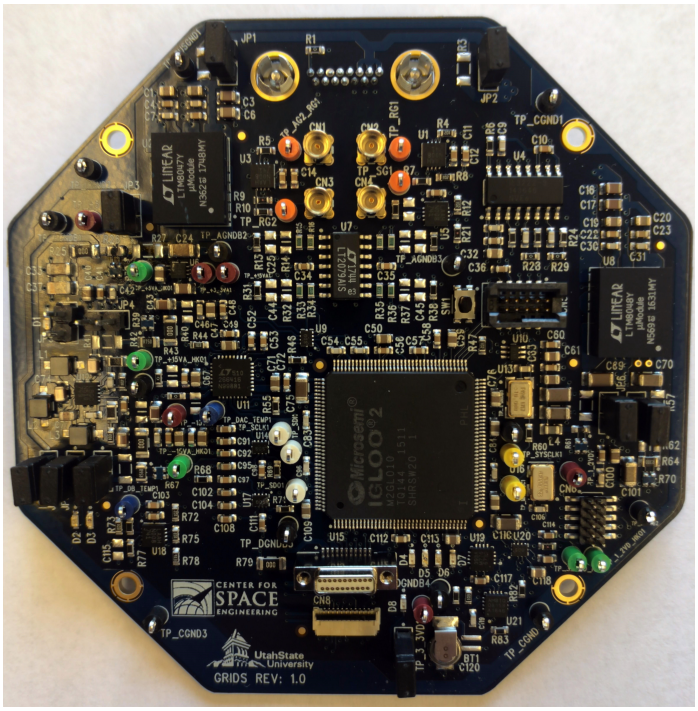

Fig. 3.1: The Completed First-Generation GRIDS Main Board

3. Over-voltage protection of the RS422 transceiver

4. Board layout changes such as a new current-sense resistor, size reduction of several two-pin headers, and increased space around connectors.

5. Manufacture of new, flight-quality, internal, coaxial cables

6. Implementation of a Cyclic Redundancy Check (CRC)

7. Correction of erroneous assignments of DAC channel outputs in firmware

8. Correction of the feedback loop that adjusts current measurement timing

9. Reduction in data clock rates for the DDC114

10. Addition of board identification to housekeeping data

Hardware Modifications

The first necessary hardware modification to the GRIDS main board was the correction of incorrect signal assignments. During debugging of the first-generation GRIDS main board, it was discovered that a mistake was made during schematic capture where two pins had been connected incorrectly. The serial-data-out pin of the RTC was connected to the chip select signal coming from the FPGA and, conversely, the chip select pin of the RTC was connected to the SPI bus shared by every IC on the board. In this configuration, every time an IC on the main board transmitted on the SPI bus, the RTC toggled between enabled or disabled. To remedy this problem, a firmware patch implementing bidirectional buffers allowed the RTC to be interfaced with. Permanent correction occurred after the schematic was updated and the second-generation of the main board was manufactured. When the second-generation board was in hand, the firmware was modified to remove the bidirectional buffers and interface with the RTC as initially intended. The rectification was successful and the RTC functioned properly. Next, after some modification of the VHDL, the RTC was updated with current date settings (year, month, day, time, etc.).

Another misplaced signal on the schematic led to a button switch being shorted across its terminals. This rendered the FPGA useless until the button was removed. The ambiguous schematic symbol was improved to clearly show the four pins on the button. The correct signals were then assigned to the pins so that the button could be used.

Second, an additional IC needed to be added to the main board. It is beneficial to give GRIDS the ability to record how many times it has been power cycled. Upon boot-up, the FPGA firmware retrieves a number from non-volatile memory. This number represents the power cycle count. It is incremented and stored back into memory. A magnetometer on the main board had some non-volatile memory which was utilized for this purpose, despite being outside the intended use of the magnetometer. It was desirable, therefore, to find a dedicated non-volatile memory. The part that was selected was the Adesto Labs AT25SF041 FLASH memory. It was selected because of its SPI interface, high number of read/write cycles, and low power consumption. The dedicated memory functionality and high number

of read/write cycles are some of the advantages of using this part. With the addition of the memory, additional firmware needed to be produced to interface with it. The code was written and the power-cycle count functionality was verified.

Third, over-voltage protection needed to be added to the five-volt power line of the RS422 transceiver. During many tests performed at Virginia Tech (VT), the RS422 IC on the main board was damaged. After replacing the IC several times, it was determined that the output inductance of the power supply used to power GRIDS was too high. This caused transients to occur on the power line of the RS422 chip which exceeded absolute maximum ratings. To ameliorate these unfavorable circumstances, the troublesome power supply was replaced and a 5.6-volt Zener diode was added between the five-volt power line and ground. The Diodes Incorporated BZT585B5V6T-7 was selected because of its small form factor, tight 2% tolerance, wide operating temperature range of -65°C to 150°C, and respectable power dissipation of 350 mW. Using this diode will effectively keep the voltage to less than the absolute maximum voltage of the part.

Several board layout changes were necessary to bring the main board to flight configuration. First, in order to measure the total power consumed by the 12-volt rail on GRIDS, a new current-sense resistor was placed on the board along with two new test points. These additions made it possible to insert a probe into the circuitry to measure input current. Second, two-pin headers on the board had to be reduced to a smaller size. The larger size protruded from the board too far and interfered with proper assembly of the GRIDS hardware. Lastly, four connectors used to drive the voltages on the grids in the grid stack needed more room around them to allow mating cables to connect and fit between the connectors. The new mating cables were made with low-outgassing heat shrink and ring terminals.

These changes required a second-generation of the GRIDS main board to be manufactured. The second-generation board is shown in Fig. 3.2 and brought the board to flight configuration.

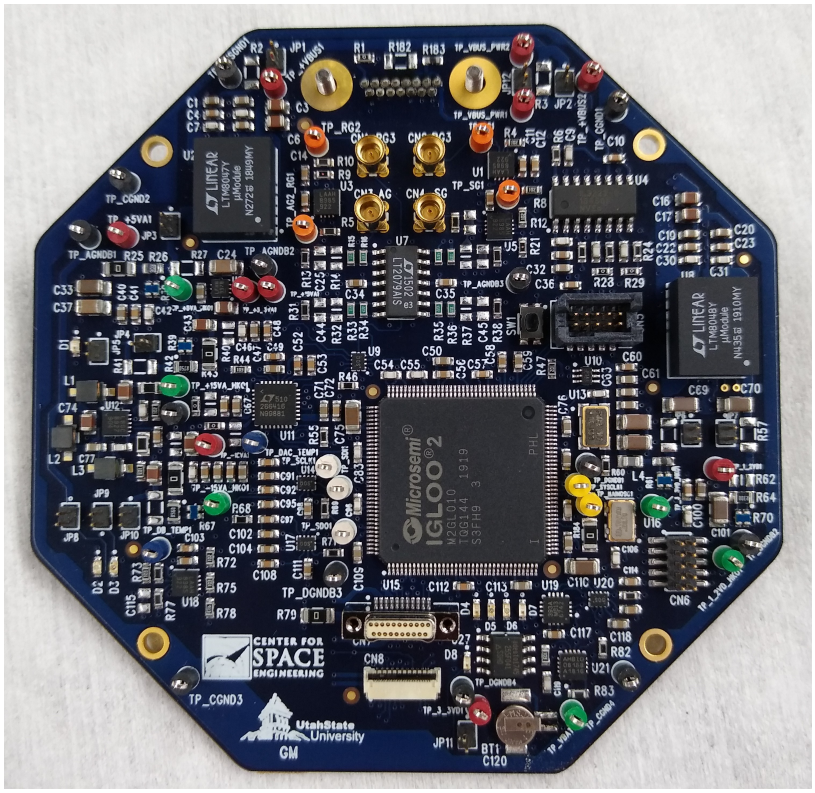

Fig. 3.2: The Completed Second-Generation GRIDS Main Board

Firmware Modifications

Accompanying the hardware changes were several firmware alterations. The changes needed were:

1. Correction of the current-ranging default value
2. New DAC output channel assignments
3. A slower data clock used to read bits from the DDC114
4. Modification of housekeeping to include identification information
5. Reprogramming the Real-Time Clock
6. Adding an interface for the new FLASH memory
7. Implementation of a Cyclic Redundancy Check (CRC) for error detection

As GRIDS flies through the upper atmosphere, the varying plasma density will be measured as a change in current. To improve the current measurements, the GRIDS firmware has current thresholds. When the measured current goes above or below these specified thresholds, GRIDS changes the amount of time it collects the incoming current. For small incoming currents, GRIDS will collect current longer than for large currents. As the sensor transitioned from RPA mode to IDM mode, however, the exact opposite behavior of what was needed was observed. Debugging this required digging through some code to find where an incorrect value was assigned. Once this was found and corrected, the RPA-to-IDM transitory behavior was nominal.

Some hardware errors created some issues for GRIDS. Due to how the GRIDS grid stack was constructed, the voltages intended for the aperture grid and one of the retarding grids were swapped. Changing the DAC output channel address assignments in firmware was a simple solution to this hardware error. A similar simple solution was implemented when clock signal integrity issues were created by a new PCB layout. To remedy this, the clock used to read bits out of the DDC114 was slowed down until all the data was successfully extracted.

Including a unique identification number within the GRIDS housekeeping provided the ability to correlate collected data to one of five copies of the GRIDS main board. This proved useful when USU and VT were testing different main boards at the same time. A link could be established between which main board produced a particular set of data.

The new flash memory added to the main board required VHDL to be written to interface with it. Code was written and its functionality verified by observing the power-cycle counter incrementing by one with each power cycle.

The last firmware modification was more involved. A 16-bit CRC needed to be implemented to detect bit errors. Implementation began by editing a VHDL module used to read data out of the FPGA's Block Random Access Memory (BRAM). The data was read out in one-byte chunks and the shifted on to the RS422 bus serially. The state machines that controlled the reading and shifting out of data had to be changed so that data could simultaneously be sent out on the RS422 line as well as through a shift register used to calculate the CRC. This permitted the CRC to be calculated on-the-fly as data shifted on to the bus. As soon as the last bit was counted and shifted out, the CRC completed its calculation by shifting 16 more zeros through the shift register and then transmitting the two-byte CRC before the next packet arrived. A VHDL testbench was written and provided a high level of confidence that the design would work as intended. Once the FPGA was programmed, verification that the CRC was correct occurred by writing a MATLAB script that parsed a GRIDS data packet which contained a CRC. The MATLAB script resulted in a CRC of all zeros indicating that the CRC calculated by the VHDL was correct.

3.1.2 GRIDS Daughter Board

The daughter board in GRIDS is home to a quad-channel current measuring IC, the DDC114. This board also required a few modifications to take it from ETU to flight configuration. The modifications were:

1. A 180° rotation of the nano-D connector used to interface with the main board.

2. Merging of ten test points into one two-by-five header.

3. Population of several zero-ohm resistors

The daughter board interfaces with the main board via a nano-D connector. The nano-D was mistakenly laid out on the PCB rotated 180° from its correct orientation. As a result, the daughter board would only mate with the main board if the whole board was rotated. This rotation made the daughter board protrude outside of the envelope in which it had to fit. While the board could still be used for some debugging, it clearly would be unacceptable as a flight design. Correcting this mistake required a new board layout and manufacture of a second revision of the board. This revision, however, did provide an opportunity to add other convenient features to the board. Ten individual test points for digital signals were merged into one two-by-five header. The header made it simpler to connect a digital logic analyzer to the test points.

Upon receipt of the second-generation daughter board, all the zero-ohm resistors were soldered on to correct a mistake made at the fabrication house. This made the board flight-ready.

3.1.3 Creation of Support Software, Hardware and Documentation

In order to appropriately test GRIDS outside of the spacecraft bus, supporting software, hardware and documentation needed to be made. This support equipment took the form of code, cables, current sources, a Faraday cage, and documentation. For example, while operating, GRIDS produces a 1,068-byte packet every two seconds. This packet is comprised of health and status, housekeeping, and current measurement information. Table 3.1 shows the complete packet structure.

Some of the tests needed to characterize GRIDS required the sensor to be left running for weeks and even months at a time. This resulted in large amounts of data that needed to be examined in order to verify that GRIDS performed as expected. To do this, cables were made to interface GRIDS with a computer and a script was written called “GRIDS Packet Parser”. The packet parser read GRIDS packets, partitioned them, converted the partitioned binary into human-readable data, and produce a multitude of plots of the data.

Table 3.1: GRIDS Packet Structure

Bytes	Description
GRIDS Packet Header	
0-3	Sync Word
4-7	Packet Counter
8-11	Power-on Counter
12-13	Packet Length
14-33	Voltage and Current Monitors
34-47	Temperatures
48-54	Magnetometer Readings
55-56	Board ID
57-63	Time
64-65	DDC Capacitor Setting
GRIDS Packet Body	
66-73	Grid Voltages
74-83	Current Measurements
84-85	Integration Timer
The structure of bytes 66-85 is repeated 49 more times.	
1067-1068	CRC

This code proved essential to understanding the accuracy of the housekeeping and current measurement data produced by the sensor.

Other tests required computer control of a precision current source used to inject simulated ion currents into GRIDS. Being able to use the computer enhanced the ability to inject diverse current waveforms into GRIDS and automated tests that required waveforms to be repeated hundreds of times or that took hours to complete. This script is called Precision Current Source Control. The code couples the masses of various ions found at the orbit altitude of GRIDS with density information from International Reference Ionosphere (IRI) model to plot the expected incoming current versus retarding grid voltage utilizing Knudsen's equations as given in Eq. 2.5. The data points that comprise the plot are then sent to the current source as an array of current values. The current is then sourced to the GRIDS collector plates where GRIDS measures the incoming current and produces the corresponding packets. The expected input waveform is then compared against the measured waveform for similarity. This is used to verify the functionality and sensitivity of the GRIDS daughter board.

In order to more accurately characterize the ability of GRIDS to measure small currents, a Faraday cage needed to be constructed to prevent Electromagnetic Interference (EMI) from coupling into the sensor. Ryan Jacobson constructed the Faraday cage from aluminum rods, sheets of copper mesh, and copper tape. It is shown in Fig. 3.3. GRIDS fits comfortably inside the cage and cables are routed through a small hole in the side. This configuration was used to test the linearity of GRIDS measurements.

In order to process any of the data collected by GRIDS, it is necessary to know the packet structure and conversions required to make the raw data useful. To this end, a processing guide was created as road map to any involved in processing GRIDS data. This processing guide is used to understand the packet structure of GRIDS and how to convert the data in it. With these tools, USU and VT could move forward on GRIDS testing knowing that data produced was processed and compared in a consistent manner.

Fig. 3.3: Faraday Cage used to Test GRIDS

CHAPTER 4

System Level Characterization Test Results

To be confident that GRIDS can accomplish its mission, hours of testing needed to be completed. The following list contains the test categories and a brief description of each of them.

1. Long-term Performance Tests

   GRIDS is expected to operate for at least 6 months. To ensure that it can fulfill this requirement, the sensor was left running for extended durations ranging from 12 hours to over a month. As the sensor ran, data packets were produced that were analyzed for anomalies in power consumption, temperature, voltages, and so forth.

2. Measurement Linearity Verification Tests

   These tests required injecting simulated ion currents into GRIDS to verify its ability to measure currents over a range. Because the injected waveform is known, the measured current waveform can be compared against. The more similar the waveforms, the more precise GRIDS measured the input.

3. Thermal Cycling Tests

   These tests involve varying the temperature of GRIDS to see how it performs. The need for these tests arose after observing strange behavior as the temperature of GRIDS increased. GRIDS was cycled between room temperature and approximately 70 °C many times.

4. Vacuum Chamber Tests

   VT has a vacuum chamber and an ion source that can simulate the space environment through which GRIDS will fly [16]. GRIDS was shipped to Virginia for these tests.

The faculty and staff at VT tested GRIDS to understand how accurately it measured the incoming angle and flux of the incoming ions.

5. In-rush Current Tests

   Throughout several tests in the vacuum chamber at VT, the RS422 communications went down. Upon inspecting the main board's RS422 IC, it was found that the IC was no longer operational and had to be replaced. This strange behavior happened many times. In an attempt to understand the root cause, in-rush testing was conducted to see what the voltage and current were on the rails that powered the RS422 chip.

These itemized tests are discussed in detail in the proceeding sections. They provide the insights into how GRIDS performs and provide the confidence that it will successfully perform its mission. All of the plots in this section were generated using the GRIDS Packet Parser code or the Precision Current Source Control code.

4.1 Long-Term Testing

Long-term tests are simple tests that, as the name implies, take a relatively long time to conduct. For the tests described in this section, GRIDS was powered on and left operating for eight weeks. Over the course of the test, the packets generated by GRIDS were collected and analyzed at least weekly. This was necessary for two reasons. The first reason was simply to verify that everything about the sensor was running fine. The second was to provide the computer with a manageable amount of data for processing. Over the entire duration of the test, more than 2.5 GB of data was created. This amount of data would increase computation time significantly. For these reasons, the plots in this section show one week's worth of data at a time. The graphs in this section include the temperature of the various locations on main and daughter boards. The graphs also present the voltage and power of the 5-volt rail. This data is generated using the housekeeping circuitry on the GRIDS main board. The housekeeping circuitry employs analog-to-digital converters that sample the voltages produced by temperature sensors, voltage regulators, and current-sensing instrumentation amplifiers. The data is then transmitted to the computer using the

test-support cables that allow GRIDS to run outside the satellite bus. The data is collected, processed, and analyzed.

Figure 4.1 shows the temperatures measured by the temperature sensors found on the main board and daughter board. The temperature measured by the sensors depends on the ambient temperature of the room, the location of the sensor on the board, and how much power is being dissipated by components adjacent to the sensor. Similar devices, such as the four ADCs, show excellent agreement on temperature. More importantly for PetitSat mission, all seven temperature sensors show similar sensitivity to temperature change. On orbit, this will provide enough information about the sensor to diagnose any issues should they arise. The cycling seen in the temperatures is caused by the environmental control in the laboratory. The graph shows that the daughter board temperature reading is noisier than the others. The temperature sensor on the daughter board is accurate to within ±1.5 °C whereas the sensors on the main board have ±0.5 °C accuracy. Additionally, the daughter board temp sensor output signal travels from the daughter board, through a nano-D connector, to the main board prior to being buffered and sampled by an ADC. This provides time for some noise to couple to the signal. The main board temperature sensors are embedded in the ADC providing the shortest path possible to the ADC for sampling.

Figure 4.2 shows the regulation of the 5-volt power rail over the course of the week. It shows slight temperature dependency as the drift in voltage can be seen to match the temperature variations. A black trend line is also shown in the figure. Noting the scale of the vertical axis, the figure shows that the voltage drift is less than 10 mV. The distinct values or "steps" seen in the figure are the different quantization levels of the ADC which appear because the range of the vertical axis is small.

Figure 4.3 presents the variation in current draw of the 5-volt rail over the course of the week-long test. As expected, the current draw is dependent upon temperature and is higher when the temperature is warm. The total variation is small - less than 2 mA.

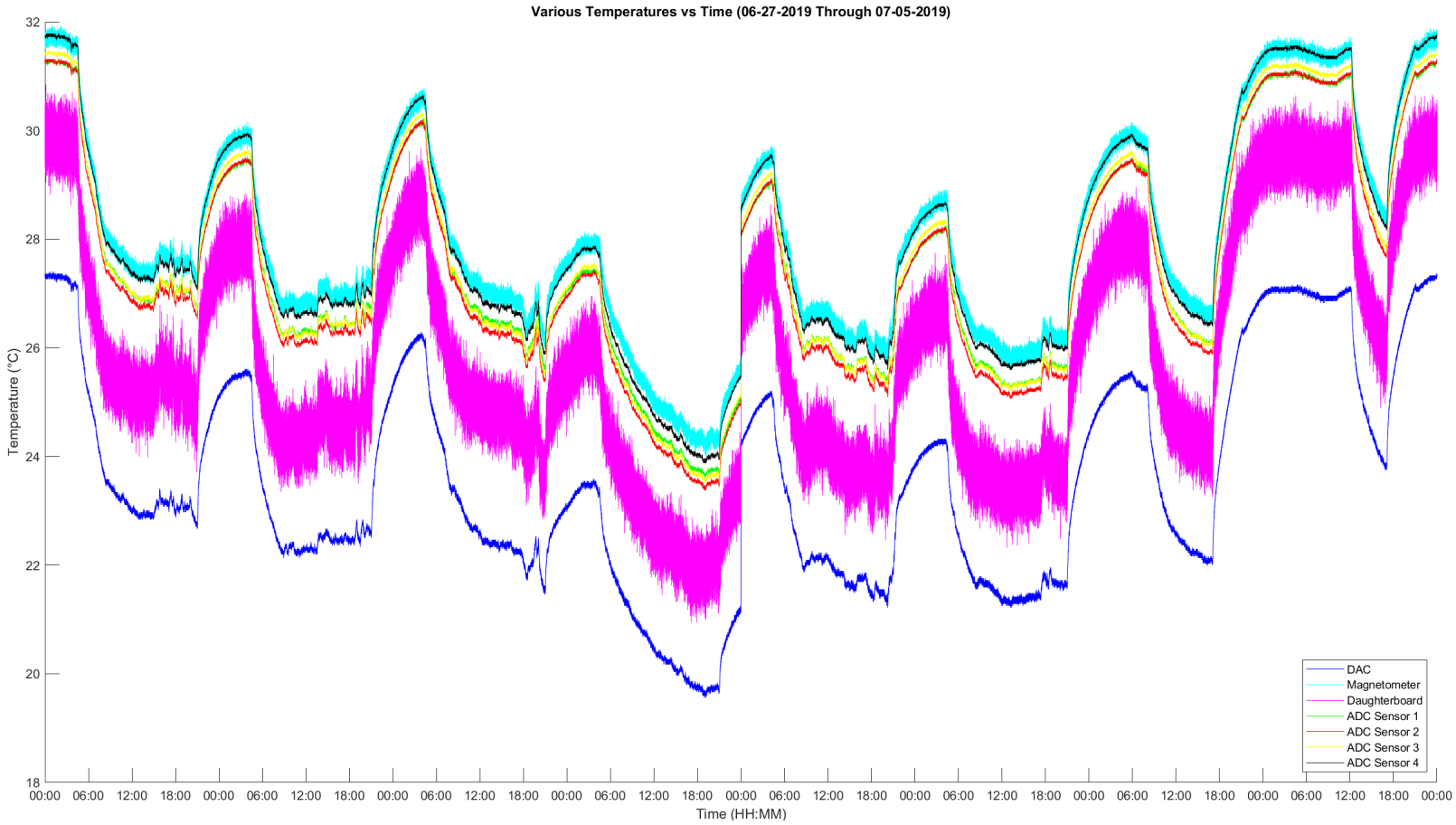

Fig. 4.1: Long-term Temperature Measurements

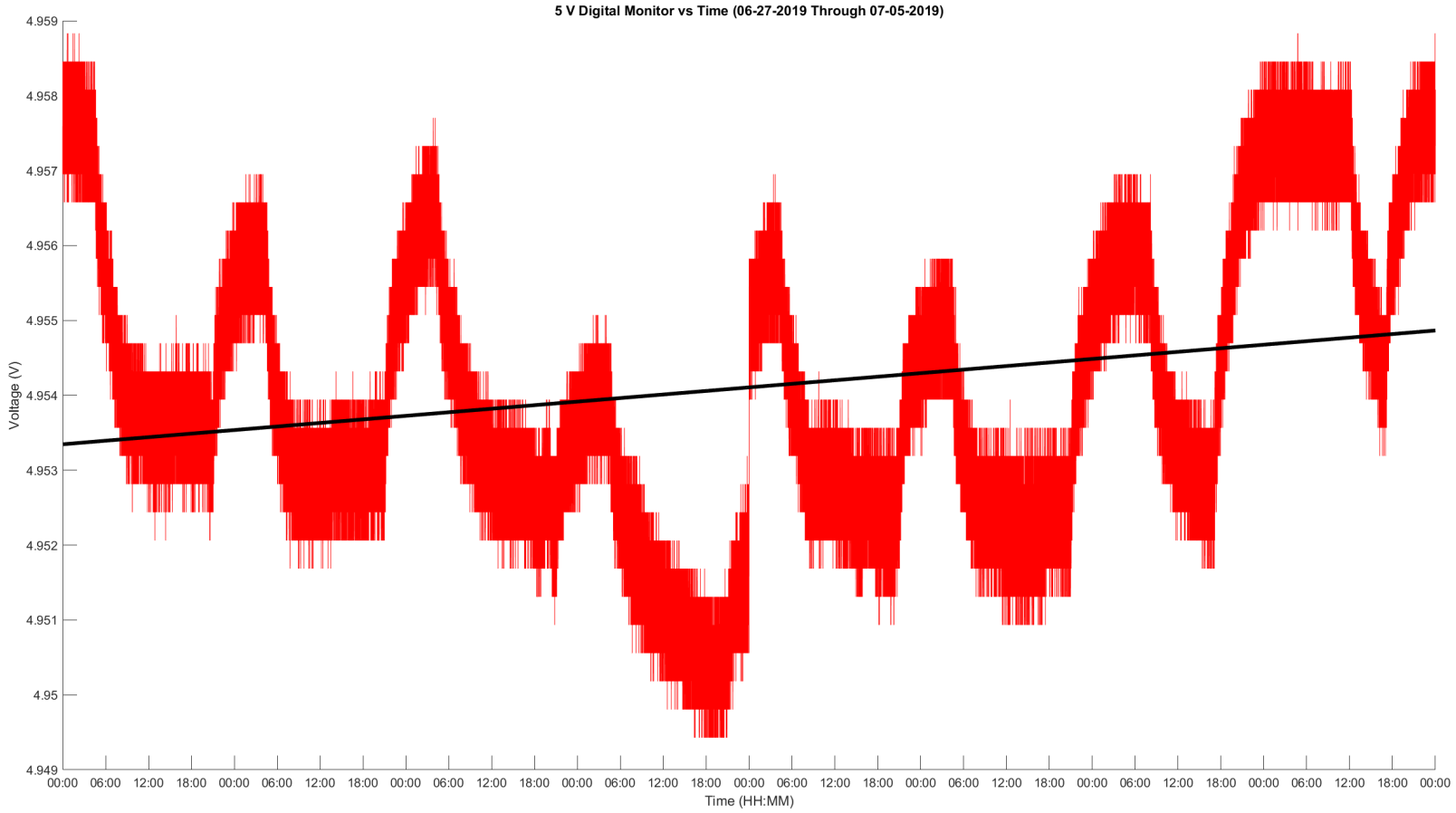

Fig. 4.2: Long-term Test 5 V Rail Measurements

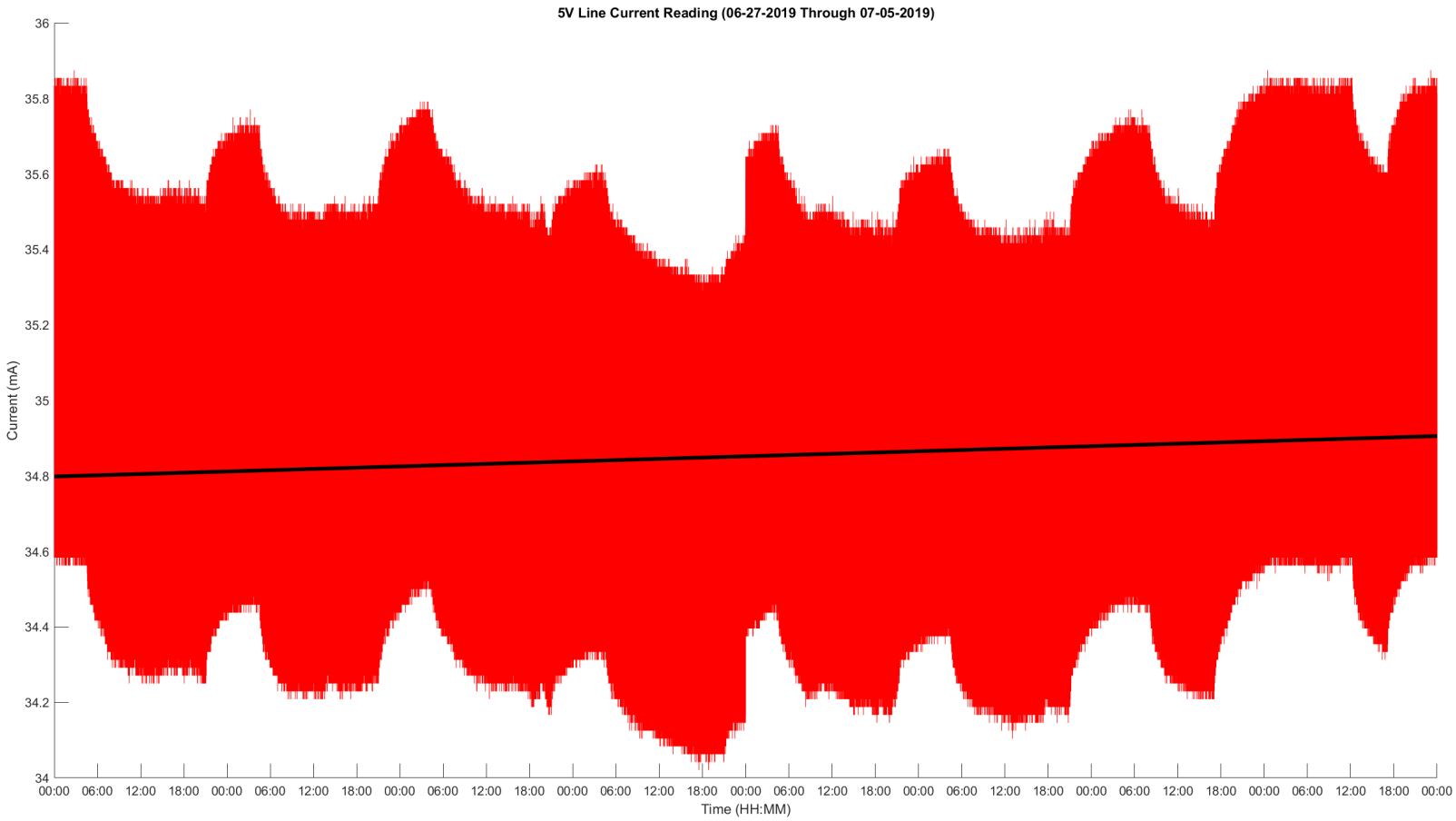

Fig. 4.3: Long-term 5 V Rail Current Measurements

4.2 Linearity Verification Testing

Proper understanding of the relationship between input current and measured current is essential to obtaining meaningful information from GRIDS. Even if the relationship is not linear, if it is consistent and repeatable then corrective measures can be taken to account for any non-linearity (i.e. calibration).

To determine whether GRIDS had any non-linearity in its current measurements, hundreds of measurements were taken at various known input currents. The collected data was then plotted. A best-fit linear regression was then performed to see how linear GRIDS measurements were. As designed, GRIDS has a highly linear relationship between its input and measured currents. The results of one such test are shown in Fig. 4.4 where the linear relationship is clear. One-hundred packets, each containing 40 measurements, were collected at each of 48 current levels on each of the four current inputs. This means a total of 768,000 points are on the graph. The best fit line is plotted and the R^2 value is shown on the graph.

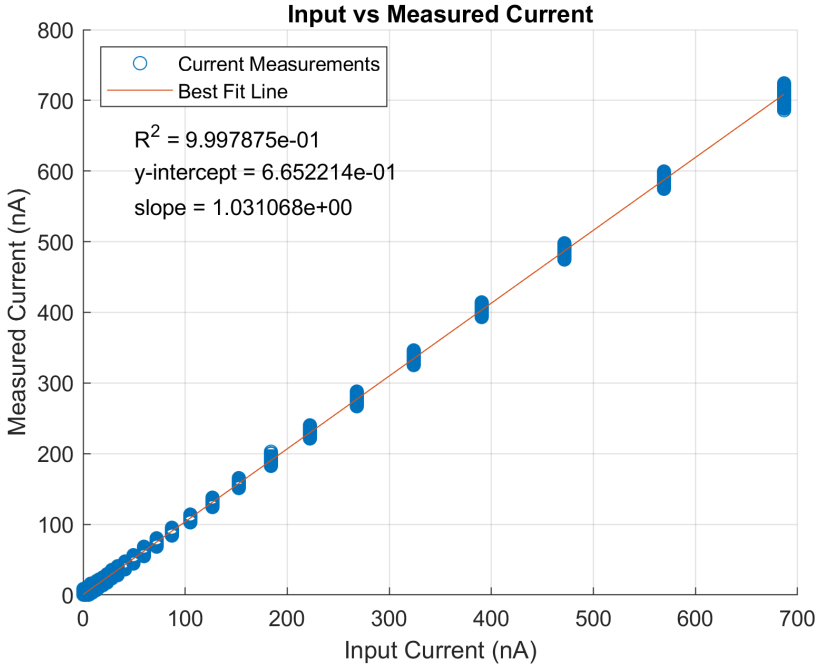

Fig. 4.4: Current Measurement Linearity

Figure 4.5 presents the standard deviation of the current measurements collected at each current level. While the standard deviation generally increases with increasing input current, it always stays below 3.3 nA.

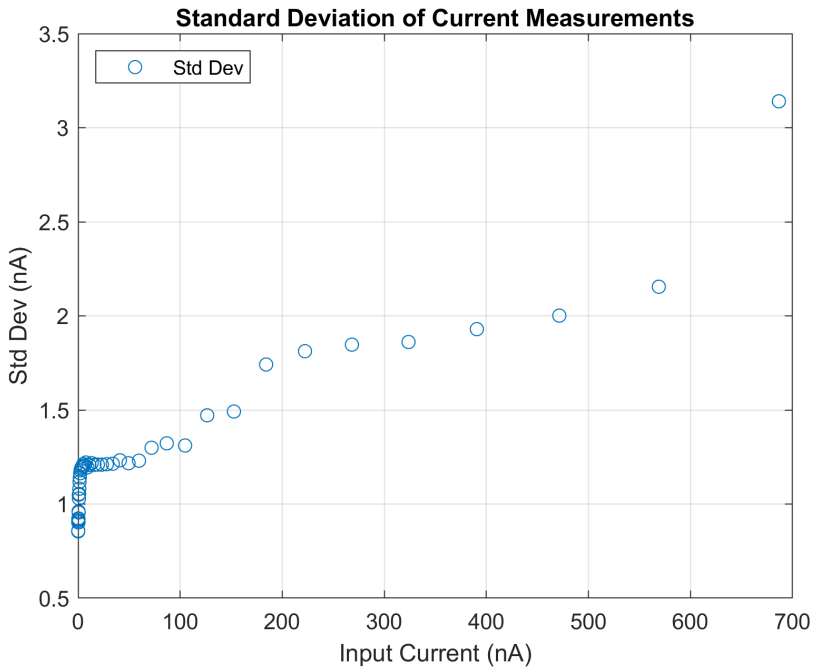

Fig. 4.5: Current Measurement Standard Deviation

With no current input and while inside the vacuum chamber (an excellent Faraday cage) at VT, the noise floor of the GRIDS current inputs is averaged to be approximately 52 pA. A plot of typical noise performance is shown in Fig. 4.6. Noise on each of the four channels as well as the summation of the noise can be seen.

4.3 Waveform Injection Tests

Many of the tests performed on GRIDS were done using a constant current input. In order to verify that the sensor can measure varying currents similar to what it will encounter on orbit, tests were performed that used the Precision Current Source Control software. Using this software allows for a wide variety of current injection waveforms to be used. An example of such a waveform is shown in Fig. 4.7. Here Knudsen's formulas [13]

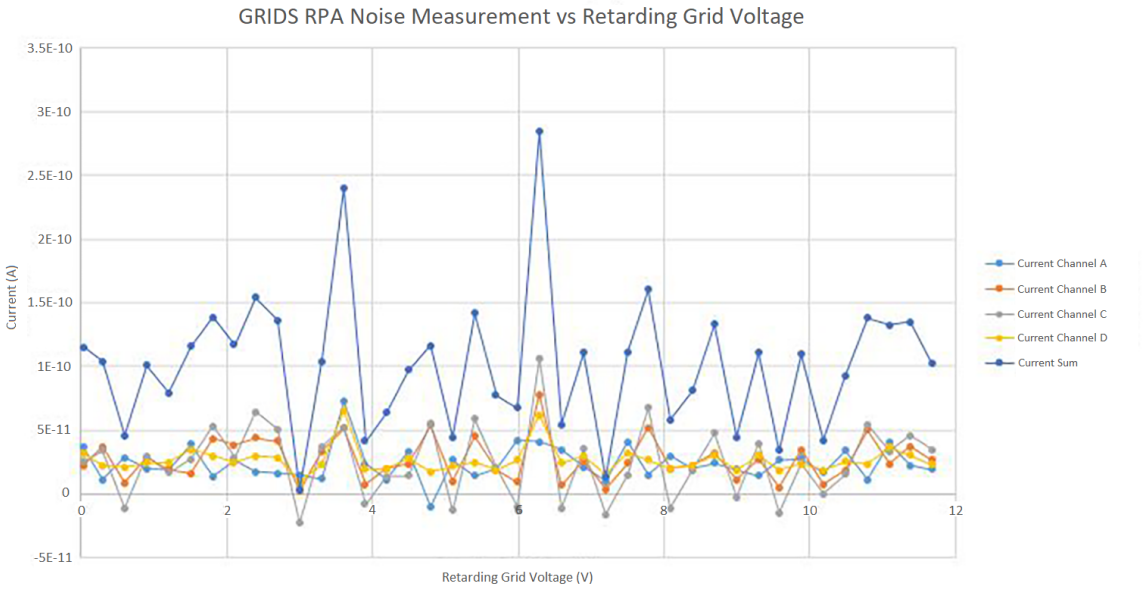

Fig. 4.6: Current Channels Noise Measurement

for an ideal RPA curve were used in conjunction with the curves found in Fanelli et al. [12]. Fig. 4.7 shows four different curves. The orange, yellow, and purple curves represent the current contribution of each ion individually. The blue curve is the summation of the other three curves. The summation or total current is the current that would be seen by the RPA on orbit. The points comprising the ideal curve shown in Fig. 4.7 are sent to the precision current source which then injects the waveform into the sensor. Figure 4.8 shows the curve reproduced from the measurements collected by GRIDS and the integration timer (the timer that tells GRIDS how long to collect current). Figure 4.8 shows that GRIDS correctly measured the input making it possible to recreate the waveform.

4.4 Thermal Cycling

During some preliminary testing in the vacuum chamber at VT, dramatic power consumption increases were observed when GRIDS warmed to above 60 °C. To diagnose the problem, the sensor was shipped back to USU where thermal cycling began in an attempt to identify the problem. A small fraction of these thermal cycles are shown in Fig. 4.9 where the increase in power consumption can be seen on every other thermal cycle. Figure 4.9

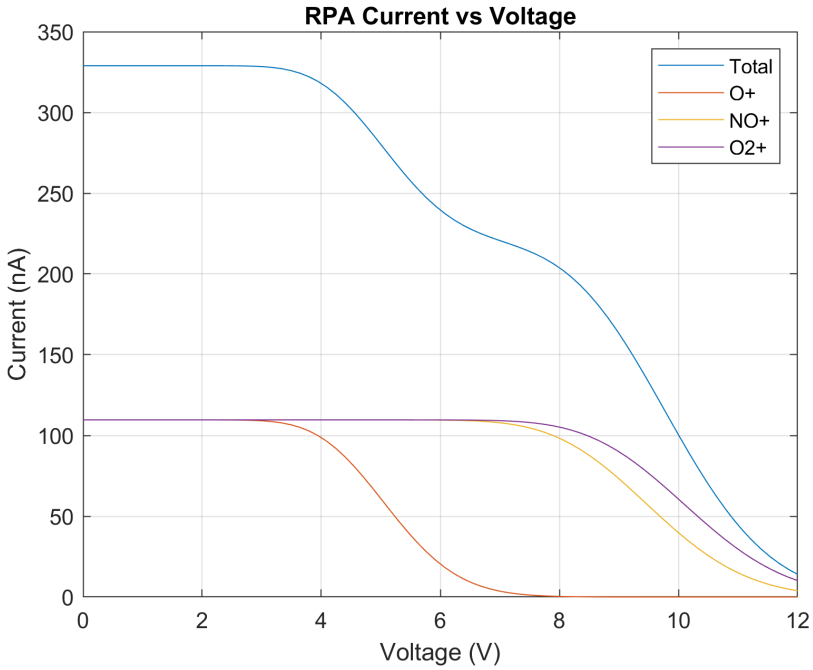

Fig. 4.7: Simulation Current Injection Waveform

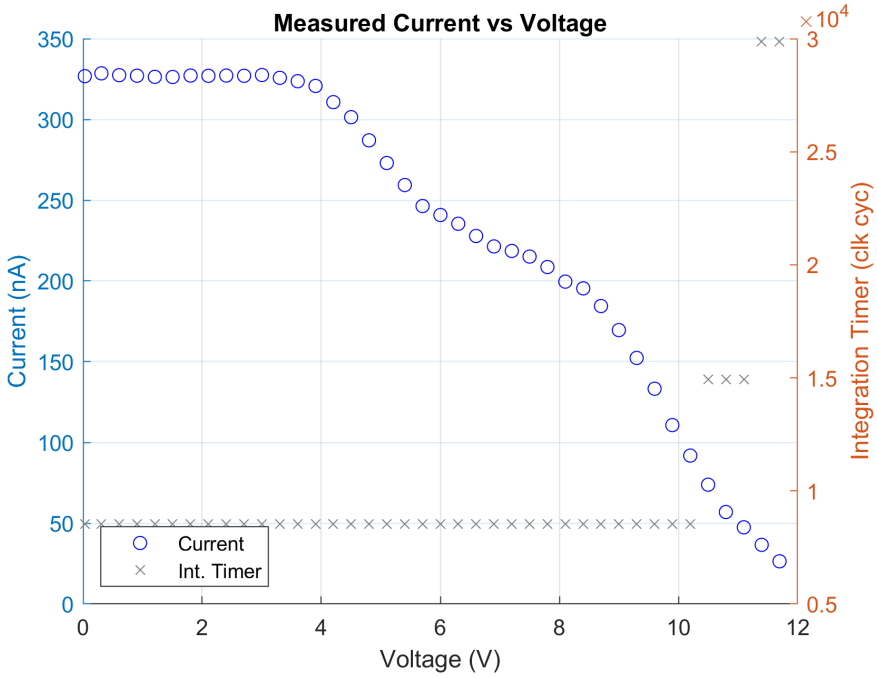

Fig. 4.8: Measured Current Injection Waveform

(a) shows the current draw on the -15 V line, (b) the current draw on the 5 V line, and (c) the measured temperature of GRIDS. The 5 V rail on GRIDS is used to power several components including an inverting boost voltage regulator. This regulator generates the -15 V line. As a result, when the current increased on the -15 V line it did on the 5 V line as well.

After examining the data and inspecting the electronics, no obvious malfunctions could be seen. This necessitated the dismantling of the entire sensor. Once the sensor's grid stack was taken apart, the culprit was visible. The plastic plate upon which the four current collection plates rested had expanded with the increase in temperature. This expansion forced the edges of the plate against the mounting screws holding it to the sensor body and its center bulged upward. When the center bulged up, the collector plates came in contact with the suppression grid. The suppression grid is held at -12 V. When the two came in contact, it caused the higher power dissipation. To fix this issue, the metal plate to which the plastic plate mounted was redesigned. The new metal plate allotted more room for expansion. Additionally, a high temperature epoxy was used to adhere the plastic plate to the metal plate. These modifications underwent several more thermal cycles and visual inspections. No increase in power consumption occurred and no physical deformation resulted.

4.5 In-rush and Functional Checkout

Over the months of testing GRIDS, several instances occurred where the RS422 transceiver in GRIDS was damaged while at VT. Knowing that proper ESD precautions were taken, the next place to look for potential causes was in-rush that occurs when the power supplies powering GRIDS are first turned on. At USU, the power supplies used had a gentle ramp that increased to 5 V, drooped, and then returned to a steady 5 V. A VT however, the power supply used drastically overshot the 5 V mark and went above 7 V before settling back to 5 V. It was this overshoot, caused by too large an output inductance, that violated the absolute maximum ratings of the RS422 IC and damaged it. After replacing the IC, a new power supply was used after verifying that it had a lower output inductance. This

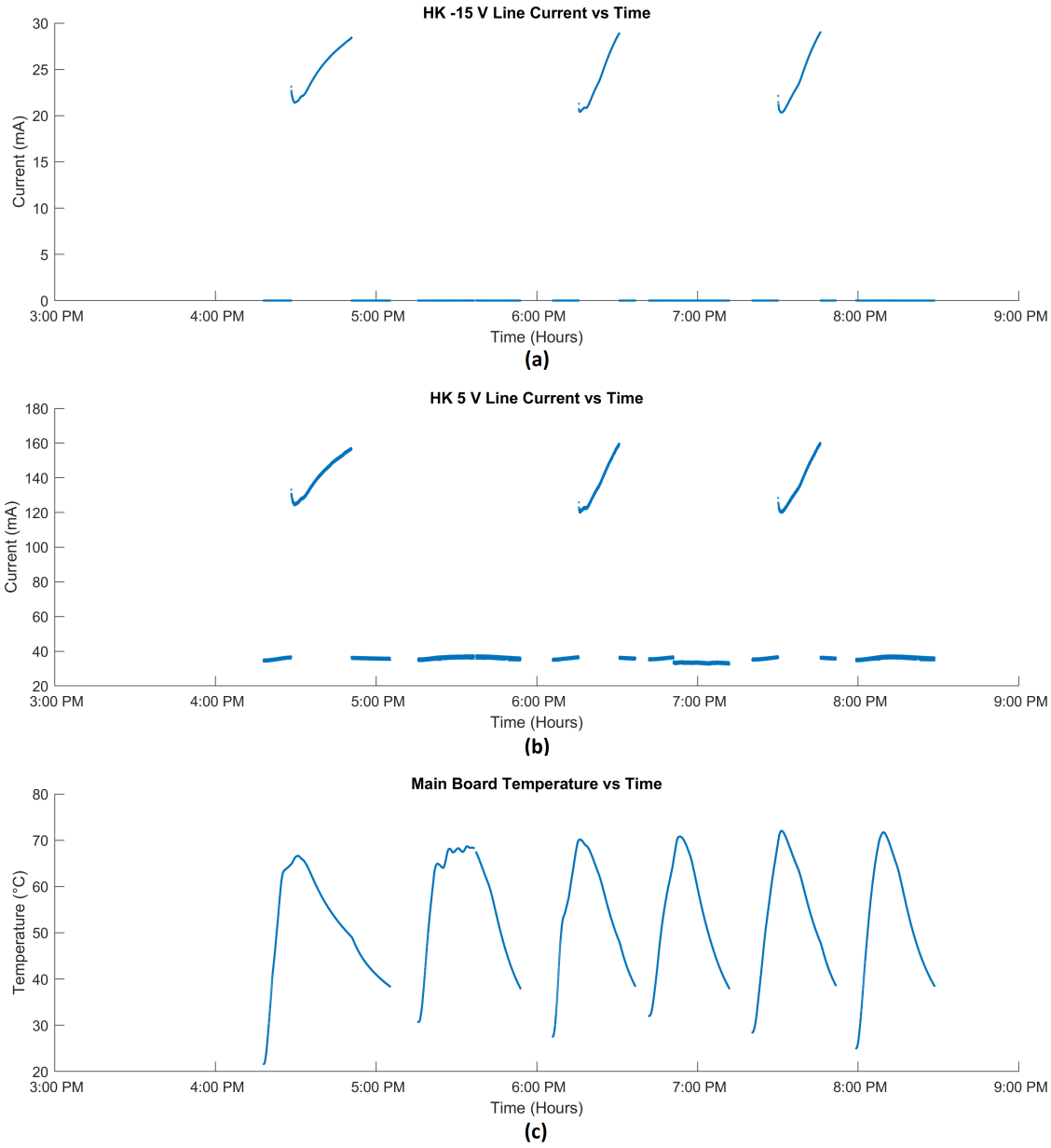

Fig. 4.9: Problematic Current Draw During Thermal Cycling

corrected the issue and kept the voltages on the RS422 IC's pins within safe operating range.

A final, simple functional checkout was performed on GRIDS prior to departing for NASA. For GRIDS this entails verifying that power consumption is nominal, correct grid voltages appear on each grid, power supply outputs are at correct, and resistances between various parts of the sensor electronics and structure are typical. This functional checkout was performed and verified that GRIDS was operational and ready to be shipped.

CHAPTER 5

Future Work and Conclusion

5.1 Future Work

There are several paths that can begin from where GRIDS concluded. In the near future, GRIDS will send data back to Earth. Significant amounts of data analysis and interpretation will be necessary. The results of this effort will produce new understanding of how ionospheric weather behaves. This information will need to be disseminated throughout the academic community allowing others to increase their understanding and generate the next iteration of hypotheses, instruments, and tests.

Additionally, though a versatile instrument, there are other future endeavors in the field of RPAs and IDMs that can utilize the work done on GRIDS. The GRIDS firmware could be enhanced with the ability to sample at different rates. This would allow GRIDS to measure wavelike ionospheric disturbances of varying wavelengths. GRIDS could also be changed to adjust not only integration time but integrating capacitors in real-time. This would enhance the precision with which GRIDS can measure varying plasma densities. Significant experience in writing VHDL could be gained by future students through rewriting portions of the GRIDS firmware to replace the automatically generated Simulink code with human written code. This would make understanding, debugging, modifying and reusing selections from the code significantly simpler.

5.2 Conclusion

This work set forth the path, obstacles, and checkpoints through which GRIDS passed to progress from a TRL 5 Engineering Test Unit to a TRL 6 Flight Unit. Hardware and firmware modifications were required as was the development of support hardware and software. Once completed, a series of tests were able to be conducted on GRIDS.

Long-term tests proved that GRIDS is capable of operating for an extended duration and maintain proper functionality. Linearity tests showed the highly linear relationship between input current and measured current. Tests measuring noise shows that GRIDS circuitry is sufficiently quiet to make very small measurements. A variety of current waveform injection tests show that GRIDS can respond correctly to changing inputs and can resolve expected waveforms with high fidelity. Heating and cooling GRIDS repeatedly in thermal cycling tests flushed out an issue with the construction of GRIDS that was then successfully remedied. After successful functional checkout, GRIDS is ready to fly aboard PetitSat and collect in-situ measurements of the ionosphere. This data will help answer the question as to whether or not there is a connection between MSTIDs and plasma enhancements.

REFERENCES

[1] V. L. Pisacane, *The Space Environment and Its Effects on Space Systems*. Reston, VA: American Institute of Aeronautics and Astronautics, 2016.

[2] M. C. Kelley, J. J. Makela, O. de La Beaujardière, and J. Retterer, "Convective ionospheric storms: A review," *Reviews of Geophysics*, vol. 49, no. 2, June 2011. [Online]. Available: https://doi-org.dist.lib.usu.edu/10.1029/2010RG000340

[3] E. S. Miller, H. Kil, J. J. Makela, R. A. Heelis, E. R. Talaat, and A. Gross, "Topside signature of medium-scale traveling ionospheric disturbances," *Annales Geophysicae*, vol. 32, no. 8, pp. 959–965, 2014. [Online]. Available: https://www.ann-geophys.net/32/959/2014/

[4] J. Klenzing, C. Clagett, R. Davidson, G. Earle, S. Jones, C. Martinis, N. Paschalidis, and R. Pfaff, "Plasma enhancements in the ionosphere-thermosphere satellite (petitsat) proposal," Aug. 2015.

[5] R. L. Davidson, B. B. Oborn, E. F. Robertson, S. Noel, G. D. Earle, J. Green, and J. Kramer, "The gridded retarding ion drift sensor for the petitsat cubesat mission," *Review of Scientific Instruments*, vol. 91, no. 6, p. 064502, 2020. [Online]. Available: https://doi.org/10.1063/1.5140470

[6] S. Jones, N. Paschalidis, M. Rodriguez, J. Sittler, E. C., and D. J. Chornay, "A Compact Ion and Neutral Mass Spectrometer for the Exocube Mission," in *AGU Fall Meeting Abstracts*, vol. 2014, Dec. 2014, pp. A23I–3354.

[7] S. Jones, N. Paschalidis, M. Rodriguez, J. Sittler, E. C., D. J. Chornay, P. Uribe, and T. Cameron, "A Compact Ion and Neutral Mass Spectrometer for Measuring Atmospheric Composition with Preliminary Results from the Dellingr Mission," in *AGU Fall Meeting Abstracts*, vol. 2017, Dec. 2017, pp. A41I–2413.

[8] E. C. Whipple, "The ion trap results in 'exploration of the upper atmosphere with the help of the third soviet sputnik'," in *Proc. IRE*, vol. 47, Jan. 1961, pp. 2023–2024.

[9] W. B. Hanson, D. R. Zuccaro, C. R. Lippincott, and S. Sanatani, "The retarding-potential analyzer on atmosphere explorer," *Radio Science*, vol. 8, no. 4, pp. 333–339, 1973. [Online]. Available: https://doi.org/10.1029/RS008i004p00333

[10] W. S. Hatch, "Plasma velocity vector instruments for small satellites," Master's thesis, Utah State University, Logan, UT, 2016.

[11] R. A. Heelis and W. B. Hanson, *Measurements of Thermal Ion Drift Velocity and Temperature Using Planar Sensors*. American Geophysical Union (AGU), 2013, pp. 61–71. [Online]. Available: https://agupubs.onlinelibrary.wiley.com/doi/abs/10.1029/GM102p0061

[12] L. Fanelli, S. Noel, G. D. Earle, C. Fish, R. L. Davidson, R. V. Robertson, P. Marquis, V. Garg, N. Somasundaram, L. Kordella, and P. Kennedy, "A versatile retarding potential analyzer for nano-satellite platforms," *Review of Scientific Instruments*, vol. 86, no. 12, p. 124501, 2015. [Online]. Available: https://doi.org/10.1063/1.4937622

[13] W. C. Knudsen, "Evaluation and demonstration of the use of retarding potential analyzers for measuring several ionospheric quantities," *Journal of Geophysical Research (1896-1977)*, vol. 71, no. 19, pp. 4669–4678, 1966. [Online]. Available: https://dx.doi.org/10.1029/JZ071i019p04669

[14] A. P. Swenson, "The field-programmable gate array design of the gridded retarding ion distribution sensor," Master's thesis, Utah State University, Logan, UT, 2017.

[15] R. A. Heelis, R. A. Stoneback, and M. D. e. a. Perdue, "Ion velocity measurements for the ionospheric connections explorer," *Space Sci Rev*, vol. 212, pp. 615–629, 2017. [Online]. Available: https://doi.org/10.1007/s11214-017-0383-3

[16] S. Dhar, "Ionospheric simulator (ionsim): Simulating ionospheric conditions in a vacuum chamber," Master's thesis, Virginia Polytechnic Institute and State University, Blacksburg, VA, 2013.